Theor Chem Acc (2015) 134:45
DOI 10.1007/s00214-015-1648-0

REGULAR ARTICLE

Revisiting the Kolbe–Schmitt reaction of sodium 2-naphthoxide

Svetlana Marković[1] · Igor Đurović[2] · Zoran Marković[3]

Received: 22 January 2015 / Accepted: 14 March 2015

Abstract The mechanism of the carboxylation reaction of sodium 2-naphthoxide (NaphONa) was investigated in the positions 1, 3, and 6 by means of three methods: B3LYP, B3LYP-D2, and M06-2X. While B3LYP failed to describe reaction pathways 3 and 6, B3LYP-D2 (owing to the empirical correction term) and M06-2X (owing to the way it has been parameterised) produced relatively consistent results which create completely new picture of the reaction mechanism. It was found that the reactants can build two NaphONa–CO_2 complexes, of which only one can be further transformed to the reaction products. In this new NaphONa–CO_2 complex, the CO_2 moiety is perfectly positioned to perform electrophilic attacks on all three nucleophilic carbons of the naphthalene ring. Each reaction pathway occurs via two transition states and one intermediate. The mechanism involves a bimolecular reaction step for proton transfer, which requires notably smaller activation barrier than previously considered intramolecular rearrangement. It was shown that reaction pathway 6 is unfavourable from both kinetic and thermodynamic points of view. On the other hand, pathways 1 and 3 are competitive: pathway 1 requires lower activation barriers, but pathway 3 yields the most stable reaction product. These thermochemical results are in good agreement with the experimentally determined products ratio.

Keywords Carboxylation reaction · Sodium hydroxy naphthoates · Mechanistic study · B3LYP-D2 and M06-2X calculations

1 Introduction

The products of a carboxylation reaction of alkali and alkaline earth metal phenoxides and naphthoxides, called the Kolbe–Schmitt reaction [1, 2], are aromatic hydroxy acids. These compounds have been successfully applied in the production of numerous important chemicals: pharmaceuticals, antiseptics, high-polymeric liquid crystals, polyesters, fungicidal and colour-developing agents, dyes, textile assistants, etc. [3–9]. Due to versatile utilisation of the aromatic hydroxy acids, the Kolbe–Schmitt reaction has been a focus of various experimental and computational researches and is still a vigorous field of investigation. A general outline of the Kolbe–Schmitt reaction of sodium 2-naphthoxide (NaphONa), the subject of the present work, is depicted in Fig. 1.

There are controversial opinions on the Kolbe–Schmitt reaction mechanism. Among several postulations of early researchers, a mechanism involving an intermediate chelate complex between carbon dioxide and metal phenoxide or 2-naphthoxide (MOPh–CO_2 and MONaph–CO_2 where M stands for a metal) is worth emphasising [1, 2, 5, 10, 11]. The presence of the intermediate PhONa–CO_2 complex was confirmed on the basis of the IR absorption spectra [12], as well as FT-IR spectra and DTA analysis [13]. The

Electronic supplementary material The online version of this article (doi:10.1007/s00214-015-1648-0) contains supplementary material, which is available to authorized users.

✉ Svetlana Marković
mark@kg.ac.rs

[1] Faculty of Science, University of Kragujevac, Radoja Domanovića 12, 34000 Kragujevac, Serbia

[2] Faculty of Agronomy, University of Kragujevac, Cara Dušana 34, 32000 Čačak, Serbia

[3] State University of Novi Pazar, Vuka Karadžića bb, 36300 Novi Pazar, Serbia

Published online: 26 March 2015

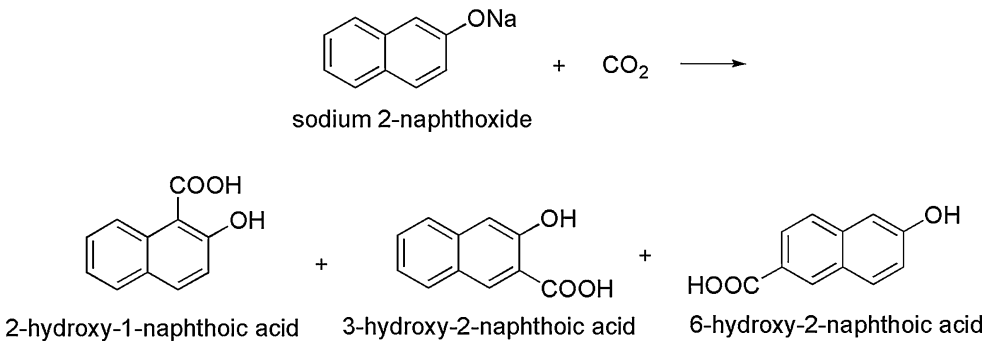

Fig. 1 General scheme of the carboxylation reaction of sodium 2-naphthoxide (NaphONa)

results of Kunert [13] indicated that direct carboxylation is not an operative mechanism of the Kolbe–Schmitt reaction.

A standpoint of initial formation of the MOPh–CO_2 or MONaph–CO_2 complex has been supported by a number of theoretical works. As for the carboxylation reaction of alkali metal phenoxides, the structure of the KOPh–CO_2 complex was elucidated [14]. It was shown that the CO_2 moiety of the MOPh–CO_2 complex performs an electrophilic attack at the benzene ring in the *ortho* and *para* positions, leading to the new intermediates and final products [14–19]. It was concluded that the introduction of the diffuse and polarisation functions does not affect the outcome of the calculations [20]. All these results refer to the monomer models where a proton shift from a carbon to the oxygen requires significantly large activation energy. Recent investigation introduced a dimer model where different behaviour of two monomers leads to notably lower activation barrier [21]. Investigation of the carboxylation reaction of 2,5-dichlorophenol indicated that higher activation barrier required for the electrophilic attack can be attributed to the electron withdrawing effect of chlorine [22, 23]. The proposed mechanism was in good agreement with the experimental results concerning the Kolbe–Schmitt reaction [24, 25]: with the NMR and IR spectra of the MOPh–CO_2 complexes, reaction temperature and pressure, equilibrium behaviour of the reaction, and ratio between the ortho and para products. Furthermore, the PhONa–CO_2 intermediate was included in some discussions on the biological Kolbe–Schmitt-like reactions [26].

There are considerably fewer theoretical results on the mechanism of the carboxylation reaction of NaphONa [27, 28]. The initial formation of the NaphONa–CO_2 complex was confirmed. It was found that the carbon of the CO_2 moiety performs an electrophilic attack on the naphthalene ring in the position 1, leading to the formation of sodium 2-hydroxy-1-naphthoate. Surprisingly, electrophilic attacks in the positions 3 and 6 were not revealed. Instead, sodium 3-hydroxy-2-naphthoate was formed by a 1,3-rearrangement of the CO_2Na group [27]. Similarly, the formation of sodium 6-hydroxy-2-naphthoate begins with an electrophilic attack on the naphthalene ring in the position 8 and is followed with a number of consecutive rearrangements [28].

A series of carboxylations of alkali and alkaline earth metal phenoxides and 2-naphthoxides provided valuable experimental information on the Kolbe–Schmitt reaction [24, 25, 29]. This reaction is very sensitive to water and is usually performed under anhydrous solvent-free conditions. Application of some solvents (tetradecane, hexadecane, trimethylphenylindane, and isopropylnaphthalene) generally leads to slowing down the reaction rate. In spite of the fact that heat distribution is more homogenised in the presence of solvents, the contact between carbon dioxide and solid substrate is decreased. It was demonstrated that the total reaction yield is governed by the pressure of CO_2 and temperature, while the products ratio is influenced by reaction temperature and time, as well as the type of alkali metal [24, 25, 29]. Some illustrative experimental results are listed in Table 1. It was shown that the total reaction yield increases with the increasing temperature [24]. At very low temperature of 293 K, only 2-hydroxy-1-naphthoic acid was obtained at small yield. The yield of 2-hydroxy-1-naphthoic acid decreased, whereas the yield of 3-hydroxy-2-naphthoic acid increased with the increasing temperature. The yield of 6-hydroxy-2-naphthoic acid was generally small (Table 1), but it was found that it can be increased by varying experimental conditions [29].

On the basis of the experimental findings, Rahim et al. and Kosugi et al. put forward a mechanism of direct carboxylation [24, 25]. The existence of the intermediate was confirmed by preparing the "pure KOPh–CO_2 or PhONa–CO_2 complex" at lower pressure. When exposed to high pressure, the complexes did not yield carboxylic acids, but the phenoxides [25]. It was concluded that, under the Kolbe–Schmitt conditions, the formation of the MOPh–CO_2 or MONaph–CO_2 complexes also takes place and is competitive with the carboxylation reactions. The experiments with a carbon-13 labelled complex, i.e. the GC/MS

Table 1 Carboxylation of potassium and sodium 2-naphthoxides with carbon dioxide at 5 MPa pressure [24]

Metal	Reaction conditions		Recovered 2-naphthol (%)	Yield (%)		
	Temp. (K)	Time (h)		2H1NA	2H3NA	2H6NA
K	293	1	47.0	52.0	0.0	0.0
K	503	10	24.0	4.0	72.0	0.0
K	523	10	10.0	2.0	87.0	0.0
Na	503	10	11.0	14.5	71.5	2.5
Na	523	10	13.0	Trace	84.5	2.0

2H1NA, 2H3NA, and 2H6NA stand for 2-hydroxy-1-naphthoic acid, 3-hydroxy-2-naphthoic acid, and 6-hydroxy-2-naphthoic acid, respectively

analysis and CP-MAS NMR spectrum of the KOPh–$^{13}CO_2$ complex, were in agreement with the direct carboxylation mechanism.

It turns out that, in spite of numerous investigations, a contradiction between the mechanism of direct carboxylation and that based on the initial formation of the MOPh–CO_2 or MONaph–CO_2 complex remains unresolved. In addition, the mechanism based on the MOPh–CO_2 or MONaph–CO_2 complex involves a reaction step with very large activation energy [14–20, 27, 28]. Finally, a mechanism of carboxylation of NaphONa in the positions 3 [27] and 6 [28] which is not based on electrophilic attacks of the carbon of the CO_2 moiety on C3 and C6 does not satisfy contemporary standards. It is worth pointing out that all theoretical works devoted to the Kolbe–Schmitt reaction [14–23, 27, 28] have been performed by using the B3LYP functional in combination with different basis sets: LanL2DZ, LAV3P**, CEP-31+G(d), and 6-311+G(d, p). Though very successful and popular, this method has failed in modelling interactions dominated by medium-range correlation energy. Motivated by the fact that more sophisticated methods are nowadays available, we decided to reinvestigate the mechanism of carboxylation of NaphONa by means of two functionals: B3LYP-D2 and M06-2X.

2 Computational details

All calculations were performed with the Gaussian 09 program package [30] using the B3LYP [31], B3LYP-D2 [32, 33], and M06-2X [34, 35] functionals. B3LYP-D2 and M06-2X were selected as widely applicable methods that proved to describe interatomic interactions at short and medium distances ($\leq$5 Å) more accurately and reliably than traditional DFT methods. Hybrid GGA B3LYP-D2 includes an empirical correction term proposed by Grimme, whereas hybrid meta-GGA M06-2X, developed by Chao and Truhlar, is characterised by the way it has been parameterised. The 6-311+G(d, p) basis set was applied for C, H, and O, whereas Def2-TZVPD basis set [36] was used for Na. These triple-split valence basis sets add the polarisation functions to all atoms and diffuse functions to the heavy atoms. Geometrical parameters of all participants in the reaction of NaphONa with carbon dioxide were optimised in vacuum. Frequency calculations were performed to determine the nature of the revealed stationary points on the potential energy surface: no imaginary frequencies for equilibrium geometries and exactly one imaginary frequency for transition states. Transition state structures were additionally confirmed by carrying out the IRC (intrinsic reaction coordinate) calculations. It was proved that each transition state connects two assumed equilibrium structures. The relative free energies and enthalpies were calculated at $T = 298.15$ K and $P = 101{,}325$ Pa. Atomic polar tensor (APT) charges were used in this work.

3 Results and discussion

The findings obtained by means of the M06-2X and B3LYP-D2 functionals are to some extent consistent, whereas those produced by using the B3LYP method are completely different. It was concluded that M06-2X generated the most robust results, particularly regarding the energies. This finding is not surprising, since the parameters for this functional were optimised to minimise the errors related to various molecular features, and not merely noncovalent interactions. For this reason, the presentation will be based on the findings from the M06-2X method. When the B3LYP or B3LYP-D2 results are considered, it will be clearly indicated.

Our investigations showed that NaphONa and CO_2 can build two NaphONa–CO_2 intermediates: **B** and **C** (Fig. 2). By analogy with the works devoted to the mechanism of the Kolbe–Schmitt reaction of the alkali metal phenoxides [14–20], structure **B** has been considered as the initial NaphONa–CO_2 complex in the carboxylation reaction of NaphONa [27, 28]. The present research revealed that **B** is yielded via a transition state (Fig. S1 of Electronic supplementary material) where the new C–O bond is being formed in an electrophilic attack of the carbon of CO_2 (APT charge = 1.314) on the nucleophilic oxygen of NaphONa

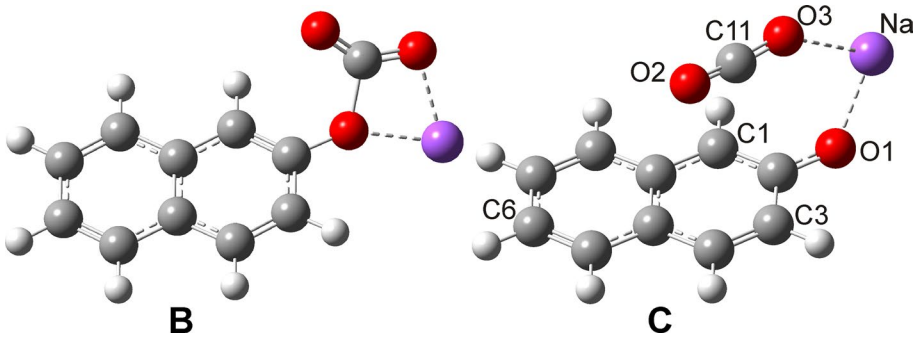

Fig. 2 Geometries of two possible NaphONa–CO_2 intermediates obtained at the M06-2X/6-311+G(d, p) level of theory (NaphONa stands for sodium 2-naphthoxide). The atom labelling scheme is presented in the structure **C**

(APT charge = −1.419). This process requires activation free energy of only 9.4 kJ mol^{-1} and is slightly endergonic (reaction free energy amounts to 2.0 kJ mol^{-1}). These facts indicate that the formation of intermediate **B** is a reverse reaction. This finding is in accord with the results of Rahim et al. and Kosugi et al. [24, 25], which showed that the formation of **B** is competitive to the carboxylation reaction. However, this complex easily decomposes to the starting compounds, while the carboxylated products are stable at higher temperatures. Since the Kolbe–Schmitt reaction is performed at elevated temperatures, the liberated naphthoxide further undergoes the carboxylation reaction.

On the other hand, intermediate **C** is built spontaneously, with small stabilisation of the system of 5.5 kJ mol^{-1}. In this intermediate, C11 of the CO_2 moiety (Fig. 2) takes an ideal position for electrophilic attacks in all three sites (1, 3, and 6). The APT partial charges on C1, C3, C6, and C11 amount to −0.431, −0.190, −0.220, and 1.251, respectively, and confirm the electrophilicity of the carbon of the CO_2 moiety and nucleophilicity of the naphthalene carbons. In addition, structure **C** is the outcome of the IRC calculations for transition state **TS1** in all three positions. These facts indicate that **C** represents the structure of the initial NaphONa–CO_2 complex that is further transformed to the carboxylation reaction products.

It is worth emphasising that transition state for the formation of **B** was not located by means of either B3LYP or B3LYP-D2. These two functionals predict that the formation of **B** is followed with a significant decrease of entropy, implying that **B** is built in an exothermic and slightly endergonic process (Table S1). Similar situation was found in the case of intermediate **C**. The structure of **C** gained by means of B3LYP requires additional comments, as it illustrates a limitation of the method to describe dispersion interactions—attractions between electrophilic C11 and carbons of the aromatic ring in this case. Namely, the C1–C11, C3–C11, and C6–C11 distances (3.305, 4. 276, and 5.937 Å) are notably longer than the corresponding distances calculated using B3LYP-D2 and M06-2X functionals (Table 2).

The mechanism of the Kolbe–Schmitt reaction of NaphONa, based on the initial intermediate **C**, is depicted in Fig. 3. The structures of the revealed transition states are presented in Fig. 4, whereas the results of the corresponding IRC calculations are depicted in Fig. S2. Interatomic distances that present evolution of bonds during the reaction course are given in Table 2.

The first reaction step is an electrophilic attack of C11 on C1, C3, or C6, which is realised via the transition states **TS1-1**, **TS1-3**, and **TS1-6** (Fig. 4). In all three transition states, a new C–C bond is being built: C1–C11, C3–C11, or C6–C11, which further leads to the formation of the corresponding intermediates **D1**, **D3**, and **D6** (Table 2). **D1** and **D2** can adopt a few isomeric structures (Fig. S3) whose interconversion occurs via low-lying transition states. Our numerous attempts to optimise **TS1-3** and **TS1-6** at the B3LYP/6-311+G(d, p) level of theory were unsuccessful, just like in the case of the B3LYP/LanL2DZ model [27, 28]. This reaction step clearly points out superiority of both M06-2X and B3LYP-D2 over B3LYP. A series of rearrangements [27, 28] is avoided by a straightforward formation of **D3** and **D6**, thus making a description of the reaction mechanism more realistic. Certainly, the key factor is the inclusion of dispersive phenomena. In the case of B3LYP-D2, this inclusion is realised via the Grimme's correction. Owing to the way it has been parameterised, M06-2X also proved to successfully describe dispersion interactions.

As for the second step of the Kolbe–Schmitt reaction, two pathways for further transformation of the intermediates **D** were examined: intramolecular shift of the proton adjacent to the CO_2Na moiety to O1 and intermolecular exchange of the protons adjacent to the CO_2Na moieties (Fig. 3). Transition states for intramolecular proton shift from C1 of **D1** and C3 of **D3** to O1 were located (Fig. S4). These transition states are very similar to those reported earlier [27, 28] and require significantly large activation free energies of 224.9 and 175.8 kJ mol^{-1}. Corresponding transition state for a proton shift from C6 of **D6** to O1 was not revealed due to notably long O1–H6 distance of 6.990 Å. In a bimolecular reaction, two **D** intermediates have to take suitable positions to build dimers **2D1**, **2D3**, and **2D6** (Table 2), i.e. reactant complexes for exchanging

Table 2 Crucial interatomic distances (Å) in the Kolbe–Schmitt reaction of NaphONa in the positions 1, 3, and 6

Distance*	Step 1			Step 2			
	C	**TS1-1**	**D1**	**2D1**	**TS2-1**	**2E1**	**E1**
	3.026	**2.056**	**1.680**	**1.544**	**1.543**	**1.498**	**1.492**
C1–C11	3.078	2.013	1.731	1.553	1.564	1.505	1.493
	3.305	*2.047*	*1.730*	*1.557*	*1.573*	*1.500*	*1.491*
	1.300	**1.263**	**1.239**	**1.209**	**1.285**	**1.348**	**1.333**
O1–C2	1.296	1.267	1.252	1.217	1.280	1.366	1.340
	1.304	*1.269*	*1.253*	*1.218*	*1.263*	*1.360*	*1.339*
	2.042	**2.104**	**2.172**	**4.963**	**4.908**	**4.502**	**4.638**
O1–Na	2.119	2.133	2.175	5.019	4.982	4.820	4.708
	2.049	*2.124*	*2.174*	*4.858*	*4.694*	*4.496*	*4.671*
	4.365	**4.249**	**4.222**	**2.191**	**2.195**	**2.265**	**2.186**
O2–Na	4.209	4.173	4.126	2.240	2.266	2.414	2.232
	4.427	*4.292*	*4.226*	*2.220*	*2.240*	*2.301*	*2.201*
				1.104	**1.366**	**4.750**	
C1′–H1′				1.101	1.517	5.565	
				1.102	*1.532*	*5.066*	
				3.385	**1.240**	**1.069**	**0.999**
O1–H1′				3.454	1.127	1.005	1.000
				5.055	*1.145*	*1.054*	*1.002*
	C	**TS1-3**	**D3**	**2D3**	**TS2-3**	**2E3**	**E3**
C3–C11	**3.426**	**1.615**	**1.550**	**1.555**	**1.560**	**1.501**	**1.496**
	3.689	1.697	1.621	1.570	1.580	1.504	1.495
O1–C2	**1.300**	**1.245**	**1.233**	**1.215**	**1.249**	**1.358**	**1.343**
	1.296	1.261	1.253	1.223	1.266	1.375	1.349
O1–Na	**2.042**	**2.216**	**2.314**	**5.045**	**4.970**	**4.586**	**4.757**
	2.119	2.220	2.269	5.047	5.042	4.863	4.813
O2–Na	**4.365**	**2.918**	**2.328**	**2.197**	**2.206**	**2.270**	**2.191**
	4.209	2.705	2.511	2.274	2.279	2.410	2.245
C3′–H3′				**1.106**	**1.313**	**4.665**	
				1.096	1.364	5.777	
O1–H3′				**2.460**	**1.350**	**1.034**	**0.983**
				2.477	1.264	0.994	0.989
	C	**TS1-6**	**D6**	**2D6**	**TS2-6**	**2E6**	**E6**
C6–C11	**5.279**	**1.632**	**1.548**	**1.554**	**1.553**	**1.506**	**1.504**
	5.087	1.622	1.560	1.571	1.572	1.504	1.504
O1–C2	**1.300**	**1.220**	**1.220**	**1.218**	**1.269**	**1.386**	**1.362**
	1.296	1.231	1.231	1.228	1.281	1.390	1.370
O1–Na	**2.042**	**4.732**	**9.717**	**9.650**	**9.760**	**10.098**	**10.325**
	2.119	5.551	9.793	9.788	9.694	10.102	10.413
O2–Na	**4.365**	**2.749**	**2.195**	**2.206**	**2.203**	**2.266**	**2.180**
	4.209	2.485	2.257	2.275	2.275	2.408	2.233
C6′–H6′				**1.106**	**1.406**	**3.683**	
				1.106	1.435	3.468	
O1–H6′				**2.372**	**1.196**	**0.970**	**0.961**
				2.503	1.191	0.985	0.963

The results obtained by means of the M06-2X, B3LYP-D2, and B3LYP methods are given in the bold, regular, and italic fonts, respectively

* The O3–Na distance varies in a very narrow range of 2.2–2.4 Å

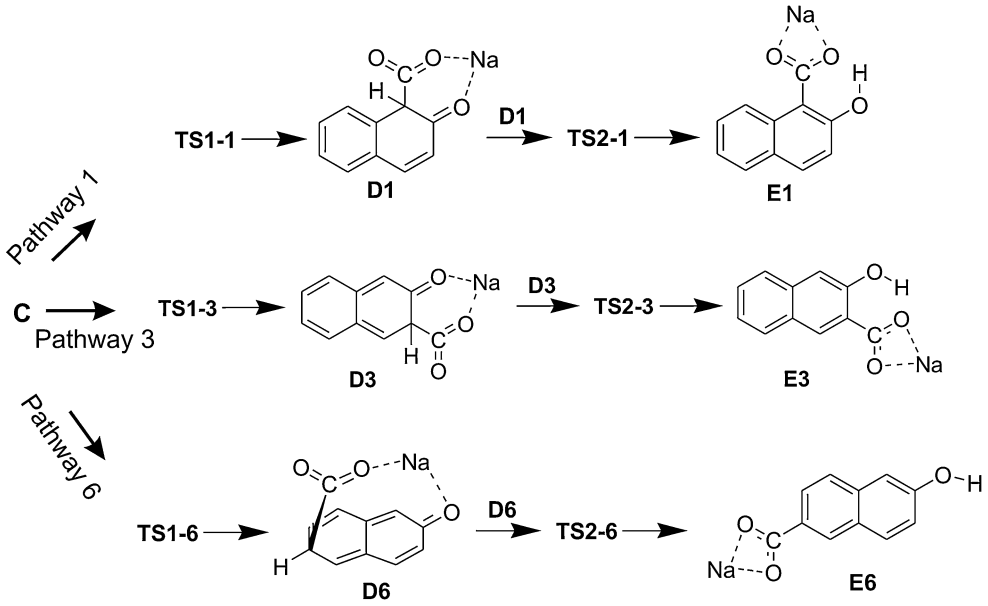

Fig. 3 Proposed mechanism for transformation of the intermediate **C** via reaction pathways 1, 3, and 6. **E1**, **E3**, and **E6** denote the reaction products: sodium 2-hydroxy-1-naphthoate, sodium 3-hydroxy-2-naphthoate, and sodium 6-hydroxy-2-naphthoate, whereas **D1**, **D3**, and **D6** represent corresponding intermediates. **TS1** and **TS2** stand for transition states in the revealed pathways

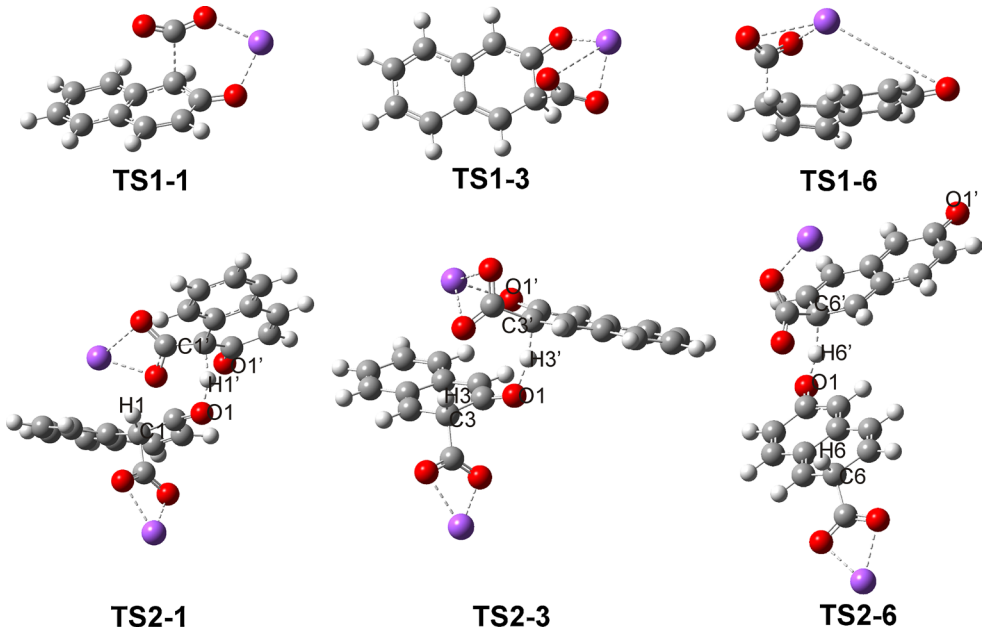

Fig. 4 Transition state structures in the Kolbe–Schmitt reaction of NaphONa in the positions 1, 3, and 6, obtained at the M06-2X/6-311+G(d, p) level of theory

the protons adjacent to the CO_2Na groups. Transition states for concerted exchange of the protons were not revealed. Instead, it was found that bimolecular reaction step occurs in a following way: O1 of **D1**, **D3**, or **D6** takes H1′, H3′, or H6′ from the corresponding **D** intermediate via transition states **TS2-1**, **TS2-3**, or **TS2-6**, respectively (Figs. 4, S5). In this way, the protonated and deprotonated forms of **D1**, **D3**, and **D6** are obtained. In the anionic **D** species, O1′ is particularly negatively charged (APT charges in the deprotonated **D1**, **D3**, and **D6** amount to −1.257, −1.295, and −1.325, respectively). At the same time, the hydrogens adjacent to the CO_2Na moieties of the cationic **D** species are partially positively charged (APT charges in the protonated **D1**, **D3**, and **D6** amount to 0.121, 0.201, and 0.203, respectively). Suitable arrangement between the cationic and anionic **D** moieties gives rise to spontaneous proton transfer (H1, H3, or H6) from a protonated structure to O1′ of the corresponding deprotonated structure (Fig. S5). In this way, the **2E1**, **2E3**, and **2E6** product complexes are built. Each of them consists of two product molecules that are associated with each other with the Coulomb and Van der Waals interactions. Our investigations showed that each pair of the **D** intermediates can exchange the protons. In Figs S6–S11 and Tables S2–S4, the reactions between

D1 and **D3**, **D1** and **D6**, and **D3** and **D6** are presented. They proceed via transition states $\mathbf{TS2_{1-3}}$, $\mathbf{TS2_{1-6}}$, and $\mathbf{TS2_{3-6}}$ and require activation energies of 61.7, 29.4, and 82.4 kJ mol^{-1}, respectively. These processes also involve spontaneous proton transfer from a protonated **D** intermediate to O1′ of a deprotonated **D** intermediate and lead to two different product molecules.

One can observe, by inspecting the values in Table 2, that B3LYP predicts notably longer O1–H1′ distance in **2D1** than other two functionals. Once again, this deviation points out the contribution of dispersion interactions on the Kolbe–Schmitt reaction. In addition, there is a small discrepancy between the B3LYP-D2 and M06-2X distances for C1′–H1′ in **2E1**, C3′–H3′ in **2E3**, and O1–Na in **TS1-6**.

Energetics of the three reaction pathways is shown in Table 3 and illustrated in Fig. 5. In spite of the fact that B3LYP-D2 systematically produces lower $\Delta G_a^{\ddagger}$ and ΔG_r values in comparison with M06-2X, the two methods exhibit similar trends. The same holds for the B3LYP results for pathway 1. As for the first step, all three pathways are endergonic. The activation energies increase in the order $\Delta G_a^{\ddagger}$(**TS1-1**) < $\Delta G_a^{\ddagger}$(**TS1-3**) < $\Delta G_a^{\ddagger}$(**TS1-6**). Very low $\Delta G_a^{\ddagger}$(**TS1-1**) value is a consequence of the pronounced nucleophilicity of C1, whereas rather high $\Delta G_a^{\ddagger}$(**TS1-6**) value can be attributed to a significant deformation of the naphthalene ring (Fig. 4; Table 2). **TS1-1** and **TS1-3** are late transition states, which is manifested through the C1–C11 and C3–C11 distances in Table 2. As a consequence, the free energies of these transition states are only slightly larger than those of the corresponding intermediates **D1** and **D3**. The C6–C11 distance in **TS1-6** is also rather short, suggesting that **TS1-6** is likewise a late transition state. However, in pathway 6, the O1–Na distance suffers significant changes, implying that in **D6** the interaction between O1 and Na diminishes, the ring becomes unstrained (Fig. S3), and, consequently, **D6** is notably stabilised in comparison with **TS1-6** (Fig. 5).

Table 3 shows that in the second step, pathway 1 requires the largest, whereas pathway 3 the smallest activation energies. However, these data are not sufficient to understand actual energy relations. The graph in Fig. 5 shows that **2D1** is the most stable reactant complex, and thus, its free energy was set to zero. We will first consider the case where the protons are exchanged between the **D** intermediates of the same kind. Here, the order of stability of the reactant complexes is as follows: ΔG(**2D1**) < ΔG(**2D6**) < ΔG(**2D3**) (the same as that of the corresponding **D** monomers). As a consequence, the highest and lowest lying transition states in the second step are **TS2-6** and **TS1-1**, respectively. In addition, the free energies of all **TS2** transition states are

Table 3 Activation ($\Delta G_a^{\ddagger}$) and reaction (ΔG_r) free energies in the first and second steps of the Kolbe–Schmitt reaction of NaphONa in the positions 1, 3, and 6

Position	Step 1		Step 2	
	$\Delta G_a^{\ddagger}$	ΔG_r	$\Delta G_a^{\ddagger}$	ΔG_r
	32.0	**26.9**	**139.3**	**−143.7**
1	26.1	24.1	101.4	−190.3
	37.3	*36.4*	*96.5*	−163.6
3	**125.1**	**119.8**	**44.2**	**−340.4**
	113.1	111.2	21.1	−375.2
6	**168.6**	**112.6**	**120.4**	**−273.4**
	166.2	103.7	90.7	−290.3

The results obtained by means of the M06-2X, B3LYP-D2, and B3LYP methods are given in the bold, regular, and italic fonts, respectively

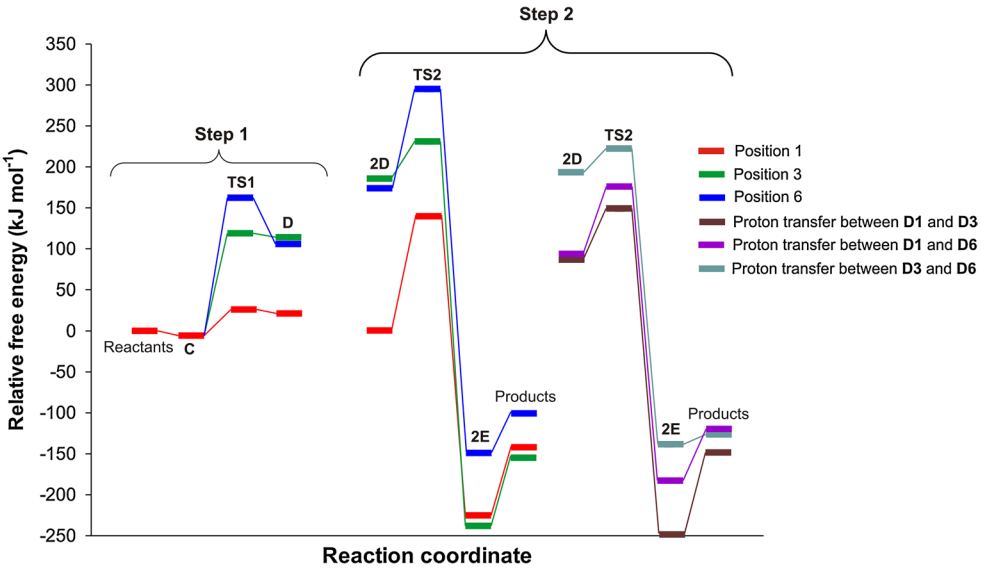

Fig. 5 Energy diagram for the carboxylation reaction of NaphONa in the positions 1, 3, and 6. In step 1, the free energy values were calculated relative to the total free energy of separated reactants (NaphONa + CO_2). In step 2, the free energy values were calculated relative to that of the reactant complex **2D1**

higher than the energies of the corresponding **TS1** transition states. It turns out that pathway 6 is unfavourable from both thermodynamic and kinetic points of view and thus leads to the minor reaction product. On the other hand, the reactions in the positions 1 and 3 are competitive: pathway 1 requires smaller activation barriers, but **E3** is significantly more stable than **E1** and **E6**. Consequently, **E3** and **E1** are obtained at high yields, where the product ratio depends on the reaction conditions.

In the case where the protons are exchanged between two different **D** intermediates, the energies of the transition states lie between those for **TS1-1** and **TS1-6** [$\Delta G(\mathbf{TS2_{1-3}}) < \Delta G(\mathbf{TS2_{1-6}}) < \Delta G(\mathbf{TS2_{3-6}})$] and do not influence the reaction kinetics. $\mathbf{TS2_{1-3}}$ is a favourable transition state and contributes to the yields of the main reaction products **E1** and **E3**. At first glance, it seems that bimolecular reaction between **D1** and **D6** is a favourable path for obtaining **E6**. However, one should bear in mind that the first step of pathway 6 requires notably large activation barrier.

4 Summary

Based on the experimental and theoretical results, a standpoint that the Kolbe–Schmitt reaction begins with the formation of the PhOM–CO_2 or NaphOM–CO_2 complex has become widely accepted. In contrast to this opinion is an assumption of Rahim et al. and Kosugi et al. on a direct carboxylation [24, 25]. Our investigation of the carboxylation reaction of NaphONa, performed by using the M06-2X and B3LYP-D2 methods, showed that NaphONa and CO_2 can build two NaphONa–CO_2 complexes: **B** and **C**. Initial complex **C** undergoes further transformation to the reaction products following three reaction pathways: 1, 3, and 6, whereas **B** decays to starting compounds when exposed to higher temperatures. All three reaction pathways take place via two transition states (**TS1** and **TS2**) and one intermediate (**D**). Recall that the B3LYP functional has not been able to locate **TS1** in pathways 3 and 6. For this reason, earlier proposed descriptions of the carboxylation reaction in the positions 3 and 6 involved a number of intramolecular rearrangements [27, 28], thus making a vague depiction of the reaction mechanism. Owing to the sophisticated parameterisation (M06-2X) and the empirical correction term (B3LYP-D2), these two methods showed much better performance in modelling interatomic interactions at short and medium distances.

It was shown that reaction pathway 6 is unfavourable from both kinetic and thermodynamic points of view. On the other hand, pathways 1 and 3 are competitive: pathway 1 requires lower activation barriers, but pathway 3 yields the most stable reaction product. The thermochemical results obtained in this study are in good agreement with the experimental findings. Namely, the yield of 6-hydroxy-2-naphthoic acid is generally small. In addition, at very low temperature of 293 K, only 2-hydroxy-1-naphthoic acid is obtained at small yield. The yields of 3-hydroxy-2-naphthoic and 6-hydroxy-2-naphthoic acids increase with the increasing temperature. The carboxylation reaction is performed at relatively high temperatures (around 500 K), and the major reaction product is thermodynamically most stable 3-hydroxy-2-naphthoic acid.

Acknowledgments This work was supported by the Ministry of Education, Science and Technological Development of Serbia, Project Nos. 172016 and 172015.

References

1. Kolbe H (1860) Über synthese der salicylsäure. Liebigs Ann 113:125–127
2. Schmitt R (1885) Beitrag zur kenntnis der Kolbe'schen salicylsäure-synthese. J Prakt Chem 31:397–411
3. Peters M, Köhler B, Kuckshinrichs W, Leitner W, Markewitz P, Muller T (2011) Chemical technologies for exploiting and recycling carbon dioxide into the value chain. ChemSusChem 4:1216–1240
4. Hölscher M, Gürtler C, Keim W, Müller TE, Peters M, Leitner W (2012) Carbon dioxide as a carbon resource—recent trends and perspectives. Z Naturforsch 67b:961–975
5. Lindsey AS, Jeskey H (1957) The Kolbe–Schmitt reaction. Chem Rev 57:583–620
6. Windholz M (1983) Salicylic acid, the Merck Index, 10th edn. Merck, Rahway, p 8190
7. Martindale W (1996) In: Reynolds JEF (ed) Martindale, the extra pharmacopoeia, 31st edn. The Royal Pharmaceutical Society, London, pp 1093–1105
8. Zevaco T, Dinjus E (2010) Main group element- and transition metal-promoted carboxylation of organic substrates (alkanes, alkenes, aromatics, and others). In: Aresta M (ed) Carbon dioxide as chemical feedstock. Wiley, Weinheim, pp 89–120
9. Matthessen R, Fransaer J, Binnemans K, De Vos DE (2014) Electrocarboxylation: towards sustainable and efficient synthesis of valuable carboxylic acids. Beilstein J Org Chem 10:2484–2500
10. Daives IA (1928) Über die bildung und den zerfall des natrium-salicylats. Z Phys Chem 134:57–86
11. Ayres DC (1966) Carbanions in synthesis. Oldbourne Press, London, pp 168–173
12. Hales JL, Jones JI, Lindsey AS (1954) Mechanism of the Kolbe–Schmitt reaction. Part I. Infra-red studies. J Chem Soc 3145–3151
13. Kunert M, Dinjus E, Nauck M, Sieler J (1997) Structure and reactivity of sodium phenoxide—following the course of the Kolbe–Schmitt reaction. Chem Ber 130:1461–1465
14. Marković Z, Marković S, Manojlović N, Predojević-Simović J (2007) Mechanism of the Kolbe–Schmitt reaction. Structure of the intermediate potassium phenoxide-CO_2 complex. J Chem Inf Model 47:1520–1525
15. Marković Z, Engelbrecht JP, Marković S (2002) Theoretical study of the Kolbe–Schmitt reaction mechanism. Z Naturforsch 57a:812–818
16. Marković Z, Marković S, Begović N (2006) Influence of alkali metal cations upon the Kolbe–Schmitt reaction mechanism. J Chem Inf Model 46:1957–1964

17. Stanescu I, Achenie LEK (2006) A theoretical study of solvent effects on Kolbe–Schmitt reaction kinetics. Chem Eng Sci 61:6199–6212
18. Stanescu I, Gupta RR, Achenie LEK (2006) An in silico study of solvent effects on the Kolbe–Schmitt reaction using a DFT method. Mol Simul 32:279–290
19. Marković Z, Marković S (2008) Last step of the para route of the Kolbe–Schmitt reaction. J Chem Inf Model 48:143–147
20. Marković S, Marković Z, Begović N, Manojlović N (2007) Mechanism of the Kolbe–Schmitt reaction with lithium and sodium phenoxides. Russ J Phys Chem 81:1392–1397
21. Yamabe S, Yamazaki S (2011) An unsymmetrical behavior of reactant units in the Kolbe–Schmitt reaction. Theor Chem Acc 130:891–900
22. Yan X, Cheng Z, Yue Z, Yuan P (2014) Synthesis of 3,6-dichloro salicylic acid by Kolbe–Schmitt reaction. 1. The primary reaction mechanism through DFT analysis. Res Chem Intermed 40:3045–3058
23. Yan X, Cheng Z, Yue Z, Yuan P (2014) Synthesis of 3,6-dichloro salicylic acid by Kolbe–Schmitt reaction. 2. Proton transfer mechanism for the side reaction. Res Chem Intermed 40:3059–3071
24. Rahim MA, Matsui Y, Kosugi Y (2002) Effects of alkali and alkaline earth metals on the Kolbe–Schmitt reaction. Bull Chem Soc Jpn 75:619–622
25. Kosugi Y, Imaoka Y, Gotoh F, Rahim MA, Matsui Y, Sakanishi K (2003) Carboxylation of alkali metal phenoxides with carbon dioxide. Org Biomol Chem 1:817–821
26. Schaarschmidt J, Wischgoll S, Hofmann HJ, Boll M (2011) Conversion of a decarboxylating to a non-decarboxylating glutaryl-coenzyme A dehydrogenase by site-directed mutagenesis. FEBS Lett 585:1317–1321
27. Marković Z, Marković S, Đurović I (2008) Kolbe–Schmitt reaction of sodium 2-naphthoxide. Monatsh Chem 139:329–335
28. Marković S, Đurović I, Marković Z (2008) Formation of sodium 6-hydroxy-2-naphthoate in the Kolbe–Schmitt reaction. Monatsh Chem 139:1169–1174
29. Ahn SJ, Lee YK (2013) Factors influencing the formation of 2-hydroxy-6-naphthoic acid from carboxylation of naphthol. J Ind Eng Chem 19:2060–2063
30. Gaussian 09, Revision A.01, Frisch MJ, Trucks GW, Schlegel HB, Scuseria GE, Robb MA, Cheeseman JR, Scalmani G, Barone V, Mennucci B, Petersson GA, Nakatsuji H, Caricato M, Li X, Hratchian HP, Izmaylov AF, Bloino J, Zheng G, Sonnenberg JL, Hada M, Ehara M, Toyota K, Fukuda R, Hasegawa J, Ishida M, Nakajima T, Honda Y, Kitao O, Nakai H, Vreven T, Montgomery JA Jr, Peralta JE, Ogliaro F, Bearpark M, Heyd JJ, Brothers E, Kudin KN, Staroverov VN, Kobayashi R, Normand J, Raghavachari K, Rendell A, Burant JC, Iyengar SS, Tomasi J, Cossi M, Rega N, Millam JM, Klene M, Knox JE, Cross JB, Bakken V, Adamo C, Jaramillo J, Gomperts R, Stratmann RE, Yazyev O, Austin AJ, Cammi R, Pomelli C, Ochterski JW, Martin RL, Morokuma K, Zakrzewski VG, Voth GA, Salvador P, Dannenberg JJ, Dapprich S, Daniels AD, Farkas O, Foresman JB, Ortiz JV, Cioslowski J, Fox DJ, Gaussian, Inc., Wallingford CT, 2009
31. Becke AD (1993) Density-functional thermochemistry. III. The role of exact exchange. J Chem Phys 98:5648–5652
32. Grimme S (2004) Accurate description of van der Waals complexes by density functional theory including empirical corrections. J Comput Chem 25:1463–1473
33. Grimme S (2006) Semiempirical GGA-type density functional constructed with a long-range dispersion correction. J Comput Chem 27:1787–1799
34. Zhao Y, Truhlar DG (2008) The M06 suite of density functionals for main group thermochemistry, thermochemical kinetics, noncovalent interactions, excited states, and transition elements: two new functionals and systematic testing of four M06-class functionals and 12 other functionals. Theor Chem Acc 120:215–241
35. Zhao Y, Truhlar DG (2008) Density functionals with broad applicability in chemistry. Acc Chem Res 41:157–167
36. Rappoport D, Furche F (2010) Property-optimized Gaussian basis sets for molecular response calculations. J Chem Phys 133:134105